Carbon 124 (2017) 152–160

Contents lists available at ScienceDirect

Carbon

journal homepage: www.elsevier.com/locate/carbon

Molecular simulation aided nanoporous carbon design for highly efficient low-concentrated formaldehyde capture

Piotr Kowalczyk [a, *], Jin Miyawaki [b, c], Yuki Azuma [c], Seong-Ho Yoon [b, c], Koji Nakabayashi [b, c], Piotr A. Gauden [d], Sylwester Furmaniak [d], Artur P. Terzyk [d], Marek Wisniewski [d], Jerzy Włoch [e], Katsumi Kaneko [f], Alexander V. Neimark [g]

[a] School of Engineering and Information Technology, Murdoch University, Perth, Western Australia, 6150, Australia
[b] Institute for Materials Chemistry and Engineering, Kyushu University, 6-1 Kasuga-koen, Kasuga, Fukuoka, 816-8580, Japan
[c] Interdisciplinary Graduate School of Engineering Sciences, Kyushu University, 6-1 Kasuga-koen, Kasuga, Fukuoka, 816-8580, Japan
[d] Faculty of Chemistry, Physicochemistry of Carbon Materials Research Group, Nicolaus Copernicus University in Toruń, Gagarin Street 7, 87-100, Toruń, Poland
[e] Faculty of Chemistry, Synthesis and Modification of Carbon Materials Research Group, Nicolaus Copernicus University in Toruń, Gagarin Street 7, 87-100, Toruń, Poland
[f] Center for Energy and Environmental Science, Shinshu University, Nagano, 380-8553, Japan
[g] Department of Chemical and Biochemical Engineering, Rutgers, The State University of New Jersey, 98 Brett Road, Piscataway, NJ, 08854-8058, United States

ARTICLE INFO

Article history:
Received 5 July 2017
Received in revised form
11 August 2017
Accepted 12 August 2017
Available online 13 August 2017

ABSTRACT

Although recent experimental studies have demonstrated that doping of nanoporous carbons with nitrogen is an effective strategy for highly diluted formaldehyde capture, the impact of carbon surface chemistry and the pore size on formaldehyde capture at ~ppm concentrations is still poorly understood and controversial. This work presents a combined theoretical and experimental study on dynamic formaldehyde adsorption on pure and oxidized nanocarbons. We find using Monte Carlo simulations and confirm experimentally that cooperative effects of pore size and oxygen surface chemistry have profound impacts on the breakthrough time of formaldehyde. Molecular modeling of formaldehyde adsorption on pure and oxidized model nanoporous carbons at ~ppm pressures reveals that high adsorption of formaldehyde ppm concentrations in narrow ultramicropores <6 Å decorated with phenolic and carboxylic groups is correlated with long formaldehyde breakthrough times measured in the columns packed with specially prepared oxidized activated carbon fiber adsorbents with the pore size of ~5 Å.

1. Introduction

Formaldehyde, an organic polar molecule with effective size ~2.5 Å and large 2.6 D dipole moment [1], belongs to a class of chemicals called carcinogenic volatile organic compounds (VOC). Formaldehyde and phenol-formaldehyde adhesives have been extensively used in many industrial applications (e.g. textile and plastic industry, automobile sector, wood processing, paints, etc.) and medical sector (biocide and disinfectant). As formaldehyde occupational exposure limit value is fixed at 0.5 ppm per 8 h [2], one needs to design efficient adsorbents capable of capturing indoor formaldehyde at extremely low concentrations (below ~1 ppm).

Recent breakthrough experiments of formaldyhyde adsorption a series of nitrogen-rich activated carbon fibers (N-rich ACF) suggest that nitrogen functionalities (e.g. pyridinic, pyrrolic, pyridonic nitrogen groups) have a dominant role during capture of highly low concentrated formaldehyde [3,4]. Lee et al. [3] concluded that an effective adsorbent for formaldehyde and other polar pollutants should contain intrinsically abundant adsorption sites for target compounds (i.e., sufficient pore volume, functional groups and adequate pore size), and hydrophobic moieties enough to repel water molecules. In another work, Lee et al. [4] found that electrospun polyacrylonitrile (PAN)-based nanofibers are superior for removing of formaldehyde at low concentrations (ca. 11 ppm) using breakthrough experiments. The observed long breakthrough times

* Corresponding author.
E-mail address: P.Kowalczyk@murdoch.edu.au (P. Kowalczyk).

http://dx.doi.org/10.1016/j.carbon.2017.08.024
0008-6223/

for a series of (PAN)-based nanofibers were explained by their tailored microporosity (pore size <1 nm, following to IUPAC [5]) and abundance of surface nitrogen groups (~18–23 wt % from the elemental analysis). PAN-based nanofibers with surface area of 1250 m^2/g and nitrogen content of 4 % wt. adsorb ~0.17 mmol/g formaldehyde. In contrast, PAN-based nanofibers with surface area of 450 m^2/g and nitrogen content of 10 % wt. adsorb ~0.43 mmol/g formaldehyde. The authors concluded that formaldehyde adsorption capacity is caused by the abundant surface nitrogen-containing groups on carbon surface, whilst the higher surface area also benefits to improve the performance of formaldehyde adsorbents [4]. Similar experimental results and conclusions were presented by other research groups [6–8]. In particular, Song et al. [8] reported a linear empirical relationship between formaldehyde adsorption and the N/C ratio. Interestingly, they did not find a relationship between the concentration of surface oxygen groups (i.e., O/C ratio) and formaldehyde adsorption capacity [8]. Similarly, An et al. [9] showed that N-doped ordered mesoporous carbon CMK-3 samples of ~3.66% nitrogen with a large specific surface area ~1600 m^2/g removed indoor formaldehyde more efficiently than pristine and oxidized CMK-3 samples. Oxidation of CMK-3 with concentrated H_2SO_4 did not significantly improve the adsorption of formaldehyde at of ~ppm concentrations [9]. Carter et al. [10] investigated the mechanism of formaldehyde adsorption on ACF and granular activated carbons (GAC). In contrast to Song et al. [8], the authors reported a correlation between formaldehyde adsorption capacity at 7–11 ppmv and the density of basic surface oxygen groups [10]. The experimental adsorption isotherms of formaldehyde vapor on GAC and ACF are classified as type V according to IUPAC [5,10]. These observations confirm that formaldehyde molecules are weakly interacting with pristine carbon surfaces, and thereby formaldehyde adsorption at very low concentrations is potentially associated with cluster formation and growth around basic oxygen-containing functional groups. However, the cluster-mediated mechanism of formaldehyde adsorption around hydrophilic adsorption centers of basicity is still poorly understood and controversial.

Experimental studies show that activated carbons having specific adsorption sites, such as, surface O- or N-containing functional groups of basicity are indispensable to remove very low concentrated formaldehyde to provide a clean air [3,4,10]. Yet, the previous studies cannot draw solid conclusions about the pore size and surface chemistry that maximize the capture of formaldehyde. It is not surprising because carbonaceous materials are both structurally and energetically heterogeneous [11–25]. The intrinsic distribution of pore sizes and diversity of various surface functional groups hamper our ability to understand microscopic details of the mechanism of dynamic formaldehyde adsorption at ~ppm concentrations. In particular, N-rich carbonaceous materials coexist with precursor-derived surface O-containing functional groups [3,4]. Moreover, irreversible chemisorption of oxygen on highly reactive sites (such as, edges and structural defects) on carbon surface is responsible for an additional doping [26,27]. In ~ppm order adsorption mineral ash (e.g. silicates and metal oxides) and other heteroatoms (e.g. sulfur, phosphorus, heavy metals, etc.) can interfere understanding of the mechanism of low concentrated formaldehyde dynamic adsorption because of the competitive adsorption at the high energetic sites [28]. Therefore, the empirical relationships between N/C or O/C ratio and the formaldehyde capacity should be taken with caution [8].

In this work we present a comprehensive study of formaldehyde dynamic adsorption on microporous carbons. Firstly, we use atomistic Monte Carlo simulations of formaldehyde adsorption in pure and oxidized carbon micropores in the grand canonical and meso-canonical ensembles to understand microscopic details of the formaldehyde adsorption mechanism from ~ppm to 2 atm. The main question to be addressed with molecular simulations is whether there are cooperative effects of pore size and oxygen surface chemistry on formaldehyde capture at ~ppm concentrations. Secondly, we bridge the molecular modeling with experiment on well-characterized pitch-based ACF. Finally, we presented conclusions and future prospects for highly efficient low-concentrated formaldyhyde capture from molecular simulation aided nanoporous carbon design.

2. Experimental details, molecular models and efficiency factor

2.1. Materials, modifications and formaldehyde breakthrough experiments

We studied two samples of pitch-based activated carbon fibers (ACF) with published pore size of 5 Å and 7 Å from the Osaka Gas Company, Japan [29–31]. We used hydrogen treatment of ACF samples to prepare two hydrogen-treated ACF samples, labelled as H-5Å and H-7Å. For this treatment, we applied about 0.8 g of each ACF to the flow of H_2/Ar with 1/4 v/v and 200 mL/min in total flow rate at 600 °C for 24 h. Additionally, we prepared two oxidized ACF samples, labelled as Ox-5Å and Ox-7Å. For this treatment, we treated ACF samples with 10% perhydrol for 3 h at room temperature. After oxidation, we filtrated, washed with deionized water to adjust pH to approximately 7, and then dried the samples. For breakthrough experiments, we used the standard dry formaldehyde gas at 20 ppm of concentration. The formaldehyde was diluted by pure nitrogen (20 ppm HCHO/N_2) and it was purchased from Asahi Sanso Company Inc., Japan. We constructed a fixed bed unit with a column of 40 mm in length and 8 mm in diameter. We loaded 100 mg of each ACF sample into the in-house apparatus (Fig. 1S in the supporting information) and we balanced the 20 ppm formaldehyde-containing standard gas with pure N_2. As previously, pure N_2 was fed into the system at a flow rate of 100 mL/min and 303 K [3,4]. Details of the CHN analysis and N_2 porosimetry measurements are given in Section 1 attached to the supporting information.

2.2. Molecular models and efficiency factor

We constructed 28 structural models of pure, phenolic- and carboxylic-rich carbon micropores with pore sizes from 3.0 Å to 20.3 Å. The first oxidized carbon model, called phenolic carbon, has 4.9 and 1.1 wt % of oxygen in phenolic and carboxylic groups, respectively (Fig. 1). The second oxidized carbon model, called carboxylic carbon, has 9.8 and 0.5 wt % of oxygen in carboxylic and phenolic groups, respectively (Fig. 1). The positions and orientations of phenolic and carboxylic groups on pore walls were generated randomly using the algorithm described elsewhere [32,33]. The microscopic slit-shaped carbon pore model without any structural defects and edges does not reflect the real molecular level morphology of micropore surfaces in ACFs. Although more realistic three-dimensional models constructed using the reverse MC technique that we used in our other works [22] better reflect the structural heterogeneity of microporous carbons, the objective of this work is to demonstrate the effects of chemical modification that are more transparent with the simplest slit-pore model. Further work may be extended to functionalized three-dimensional carbon models.

For each pore width, $H = H_{cc} - 3.4$ Å (where H_{cc} is the pore width defined as the distance between the plane passing through all carbon atom centers of the outermost layer of the one wall and the corresponding plane of the opposite wall, Fig. 1), we defined and

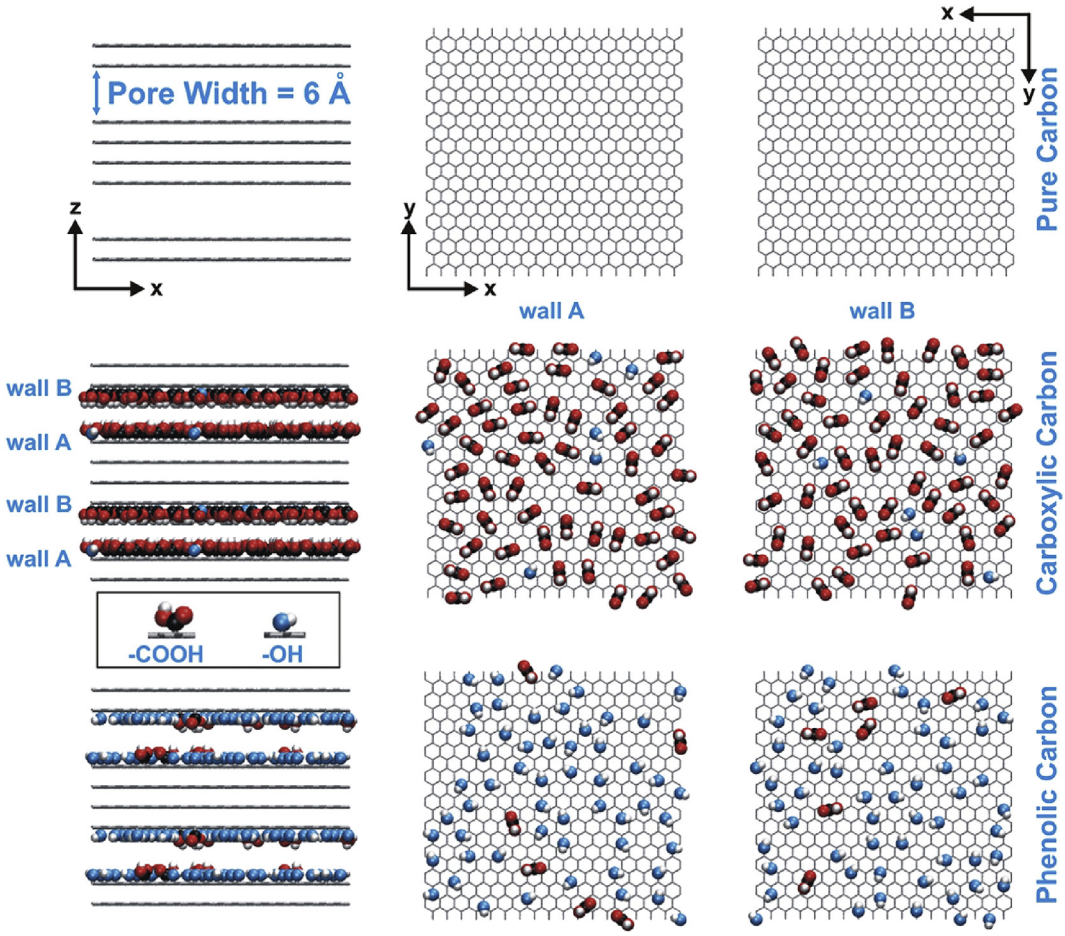

Fig. 1. Atomistic structural models of pure (top panel) and oxidized (middle and bottom panel) carbons used for systematic investigations of microscopic mechanism of formaldehyde adsorption at zero-coverage and finite pressures (i.e., ranging from ~ppm to 2 atm) at 303 K. Carboxylic carbon has 9.8 and 0.5 wt % of oxygen in carboxylic and phenolic groups, respectively. Phenolic carbon has 4.9 and 1.1 wt % of oxygen in phenolic and carboxylic groups, respectively. It should be noted that the graphics collected in this figure, Figs. 2 and 5, and Figs. 2S–5S in the supporting information are created using the VMD program [34]. (A colour version of this figure can be viewed online.)

computed the efficiency factor, $\alpha(H)$, which is a measure of the effectiveness of binding of formaldehyde to oxidized carbon ('ox') over pure carbon ('p') [35]:

$$\alpha(H) = \frac{K_{ox}(H)}{K_p(H)} \tag{1}$$

where $K_{ox}(H)$ and $K_p(H)$ corresponds to the Henry constants computed for formaldehyde adsorbed in oxidized and pure carbons at 303 K, respectively. Note that oxygen containing functional groups excluded some volumes close to pore walls, and thus pore width accessible for formaldehyde molecules is decreasing for oxidized slit-shaped carbon pores. To compare theoretical results for pure and oxidized carbons, we used pore width defined above consistently throughout the paper. We computed the Henry constant from the statistical mechanical expression using in-house Metropolis-Ulam Monte Carlo algorithm with OPLS-AA force field (Section 2.1 and 2.4 in the supporting information) [36,37]. For selected pore widths, e.g. 3.8, 5.0, 6.0, 7.2 and 10 Å, we constructed the theoretical adsorption isotherms (including: stable, metastable and unstable states) and isosteric heat of formaldehyde adsorption in pure and oxidized carbons using the grand canonical (GCMC) [38] and the gauge cell meso-canonical (MCMC) [39,40] Monte Carlo techniques at 303 K (Section 2.1.-2.3 in the supporting information). From the equilibrium GCMC configurations of adsorbed formaldehyde, we computed the average number of hydrogen bonds (H-bonds) [41,42] and the X-ray total pair correlation functions (TPCF) of adsorbed formaldehyde using canonical Monte Carlo method and Debye model [43,44] (Sections 2.5.-2.6 in the supporting information).

3. Results and discussion

Fig. 2 presents the pore width dependence of the efficiency factor of formaldehyde adsorbed on oxidized over pure carbons computed at zero-coverage at 303 K. For both carboxylic and phenolic carbons, the efficiency factor diminishes in pores larger ~7.0 Å and drastically increases in ultramicropores showing a pronounced maximum at ~5.8 Å for carboxylic carbons and ~3.0 Å for phenolic ones. The secondary well defined maximum at ~4.2 Å is also observed for phenolic carbons. The efficiency factor in carboxylic 5.8 Å ultramicropores reaches ~$5.3 \cdot 10^4$, because formaldehyde molecules (the hydrogen bond donors) are able to form H-bonds with carboxylic groups (the hydrogen bond acceptors, see GCMC snapshots, Fig. 2, left panels). Narrow phenolic 3.0–4.2 Å ultramicropores are also quite selective (although by the order of magnitude lower) with efficiency factor of ~$3.4 \cdot 10^3$-$2.3 \cdot 10^3$. From GCMC microscopic snapshots (Fig. 2, right panels), it is evident that formaldehyde molecules are forming H-bonds with phenolic groups. Moreover, specific orientation of formaldehyde imposed by

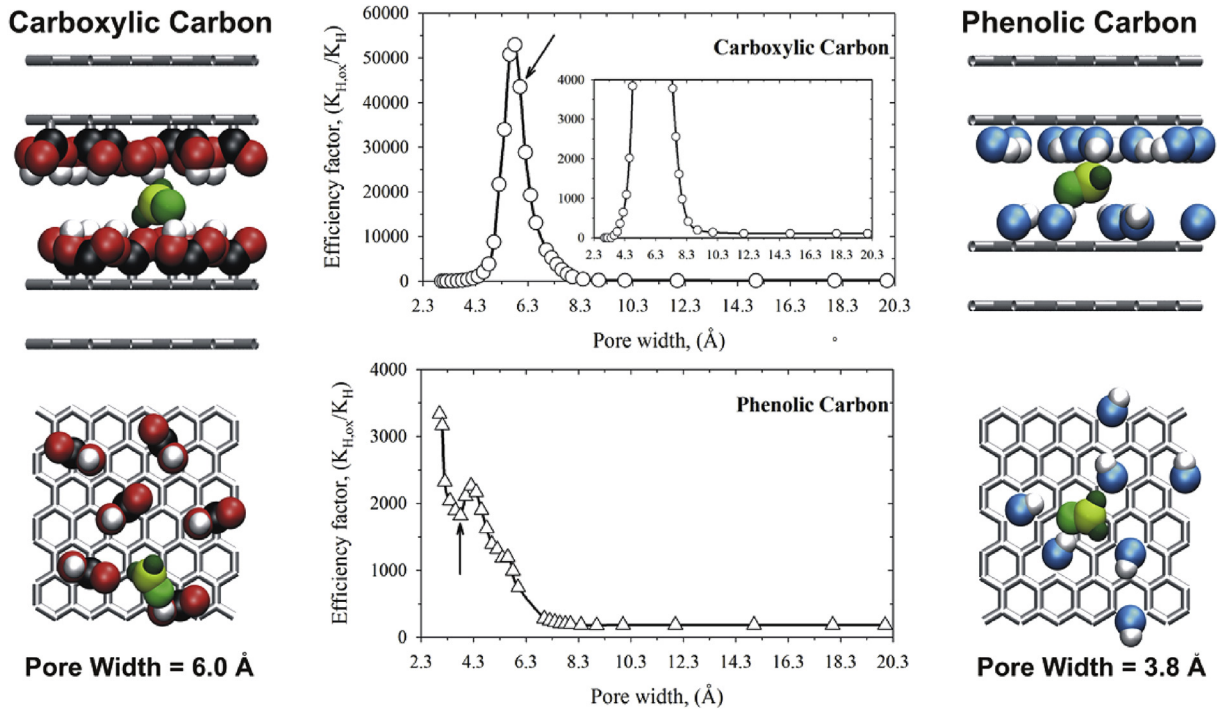

Fig. 2. The formaldehyde (α - eq. (1)) adsorbed on carboxylic (upper panel) and phenolic (bottom panel) carbons over pure carbons computed at zero-coverage and 303 K. (A colour version of this figure can be viewed online.)

phenolic pore walls influences the efficiency factor in narrow ultramicropores. Thus, we conclude that oxygen-containing functional groups, either phenolic or carboxylic, have profound impact on the efficiency factor but only in a narrow range of ultramicropore sizes. The effective size of formaldehyde molecule is ~2.5 Å [1]. Thus, it is clear that oxidation of wider micropores and mesopores with pore width ~>8 Å (i.e., pore widths accommodating more than two absorbed layers of formaldehyde, Figs. 2S–5S in

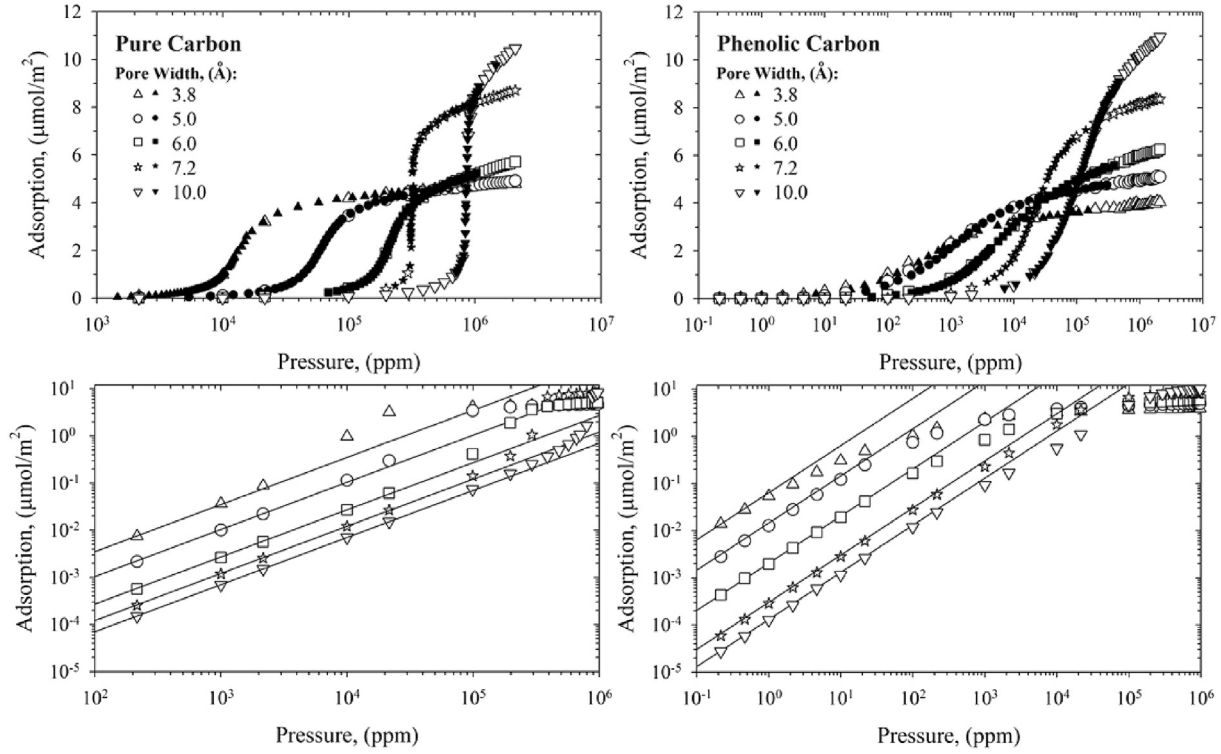

Fig. 3. Upper panels display formaldehyde adsorption isotherms in pure and phenolic carbons simulated from GCMC (open symbols) and MCMC (closed symbols) techniques at 303 K. Bottoms panels present comparison between GCMC and Henry adsorption isotherms (solid lines) at very low pressures.

the supporting information) has a negligible impact on the capturing of highly diluted formaldehyde. As we show later, in larger micro- and mesopores formaldehyde molecules that are in the contact layers are able to form H-bonds with oxygen-containing functional groups only.

To investigate the impact of phenolic and carboxylic groups on capturing of highly diluted formaldehyde in the wide range of pressures, we compute continuous formaldehyde adsorption isotherms in pure and oxidized 3.8, 5.0, 6.0, 7.2 and 10 Å micropores (Fig. 3 and Figure 6S in supporting information). In agreement with recent experiment by Carter et al. [10], we find that adsorption of formaldehyde in oxidized carbons with narrow ultramicropores starts at very low pressures of ~1–10 ppm, and the linear Henry isotherm breaks down at ~10–100 ppm (bottom panels on Fig. 3 and Figure 6S in the supporting information). The isosteric heat of adsorption in oxidized 3.8 Å ultramicropores extrapolated to zero-coverage ~65–69 kJ/mol is continuously decreasing with pore loading because the high energetic adsorption centers (spaces around functional groups) are gradually filled by adsorbed formaldehyde (Fig. 4). Interestingly, in 3.8 Å ultramicropore preferentially oxidized with carboxylic groups, the isosteric heat of adsorption is lower compared to wider 5.0 and 6.0 Å carboxylic ultramicropores. This anomalous result can be explained by steric constraints generated from carboxylic groups deposited randomly on pore walls. Note, however, that in oxidized 10 Å supermicropores the isosteric heat of adsorption extrapolated to zero-coverage drops to ~40–45 kJ/mol. The energetic effect of adsorption is drastically reduced because most of formaldehyde molecules are not able to form high-energetic H-bonds with oxygen-containing functional groups (Fig. 5S in the supporting information). At higher pressures, the adsorption isotherms are smoothed out by "rough" surface of hydrophilic pore walls (right panels on Fig. 3 and Figure 6S in the supporting information). On the contrary, in pure carbons, the adsorption uptake of formaldehyde at ~$<10^3$ ppm concentrations is negligible because there are no specific energetic sites on the graphitic walls that are targeted by formaldehyde molecules (bottom panels on Fig. 3). The isosteric heat of formaldehyde in pure carbons extrapolated to zero-coverage ~15–30 kJ/mol is continuously increasing with pore loading, indicating dominance of fluid-fluid over solid-fluid interactions (Fig. 4). In wider supermicropores, we observe the formation and growth of formaldehyde films followed by the step-like condensation. It is interesting that formaldehyde is filling supermicropores in a step-wise fashion, similarly to the first-order vapor-liquid phase transitions [45]. The formaldehyde adsorbed amount before the filling step is quite small, as similar to water adsorbed in carbon materials [30,46–51]. In strict contract to water adsorption, the nucleation energy barrier (i.e., the size of the metastability region) for vapor-liquid transition of formaldehyde in supermicropores is negligible, indicating barrier-free nucleation and spontaneous filling of pure and phenolic supermicropores at ~10^4 and 10^2–10^3 ppm, respectively (top right panel in Fig. 3).

To explore the H-bonding of formaldehyde with phenolic and carboxylic groups, Fig. 5 presents the number of H-bonds per formaldehyde molecule in phenolic and carboxylic carbons as a function of adsorbed amount at different pore widths. The number of H-bonds per formaldehyde molecule in phenolic carbons monotonically decreases with adsorption following the same trend disregarding of the pore width (Fig. 5, top panel). At low pore loadings, all formaldehyde molecules form H-bonds with phenolic groups, that corresponds to the large efficiency factor of formaldehyde adsorbed in narrow ~3.0–4.2 Å ultramicropores (Fig. 2). The H-bonding of formaldehyde with carboxylic groups depends strongly on the pore width. Snapshots of the GCMC simulations show the mechanistic basis for an excluded volume effect in narrow ultramicropores, the carboxyl groups generate inaccessible spaces, and small formaldehyde clusters are adsorbed in unoxidized parts of ultramicropores (Fig. 5, bottom panel and Fig. 2S, middle panel in the supporting information). The large peak of formaldehyde efficiency factor computed for ~5.8 Å ultramicropore with pore walls oxidized with carboxylic groups corresponds to an optimal packing of formaldehyde (Fig. 2), where the number of H-bonds per formaldehyde molecule is ~1 at low pore loadings (data for carboxylic 6.0 Å ultramicropore, Fig. 4, bottom panel). Widening or narrowing the size of carboxylic micropores lead to reduction of the efficiency factor because the excluded volume effect in narrow micropores and screening of carboxyl groups by contact layers of adsorbed formaldehyde in wider micropores, respectively. This explains the maximum of efficiency factor observed in carboxylic carbon at

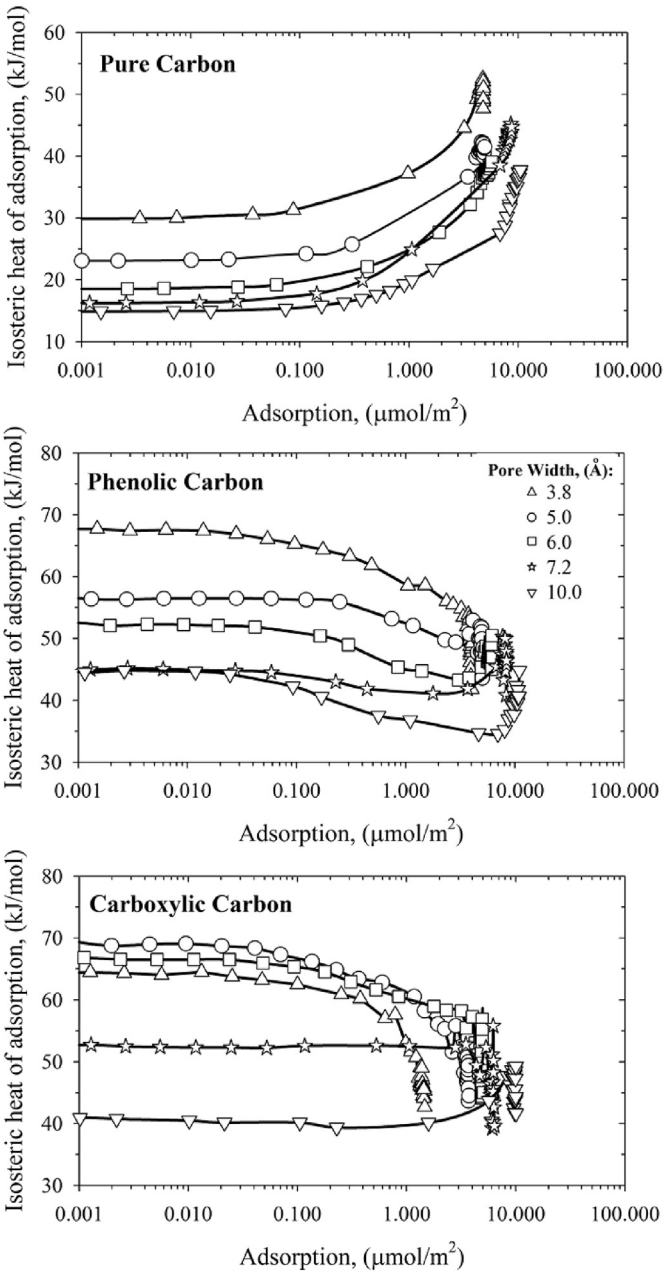

Fig. 4. Isosteric heat of formaldehyde adsorption in pure (top panel), phenolic (middle panel) and carboxylic (bottom panel) carbons computed from thermal fluctuations [35] at 303 K.

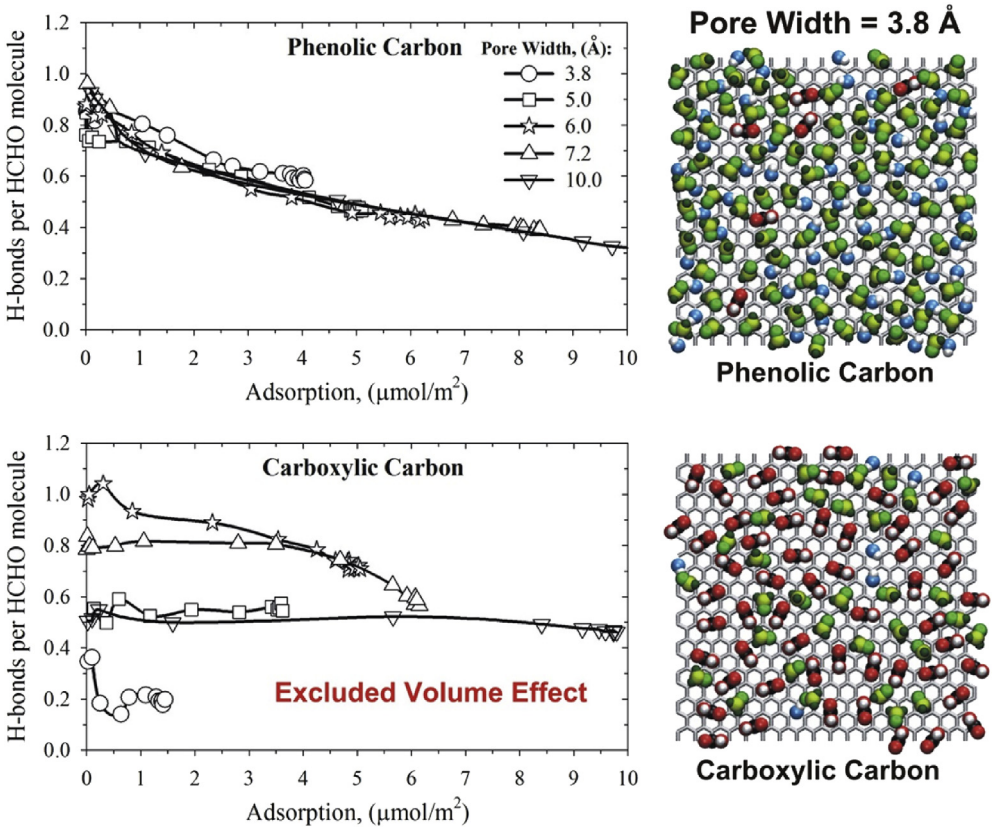

Fig. 5. Left panels present the micropore-size variation of the number of H-bonds per formaldehyde molecule adsorbed in 3.8, 5.0, 6.0, 7.2 and 10 Å oxidized carbons at finite micropore loading and 303 K. Right panels present equilibrium GCMC snapshots of formaldehyde adsorbed in oxidized 3.8 Å ultramicropores at 2 atm and 303 K. Note the number of H-bonds per formaldehyde molecule in 3.8 Å carboxylic ultramicropores is only ~0.4 due to excluded volume effect. (A colour version of this figure can be viewed online.)

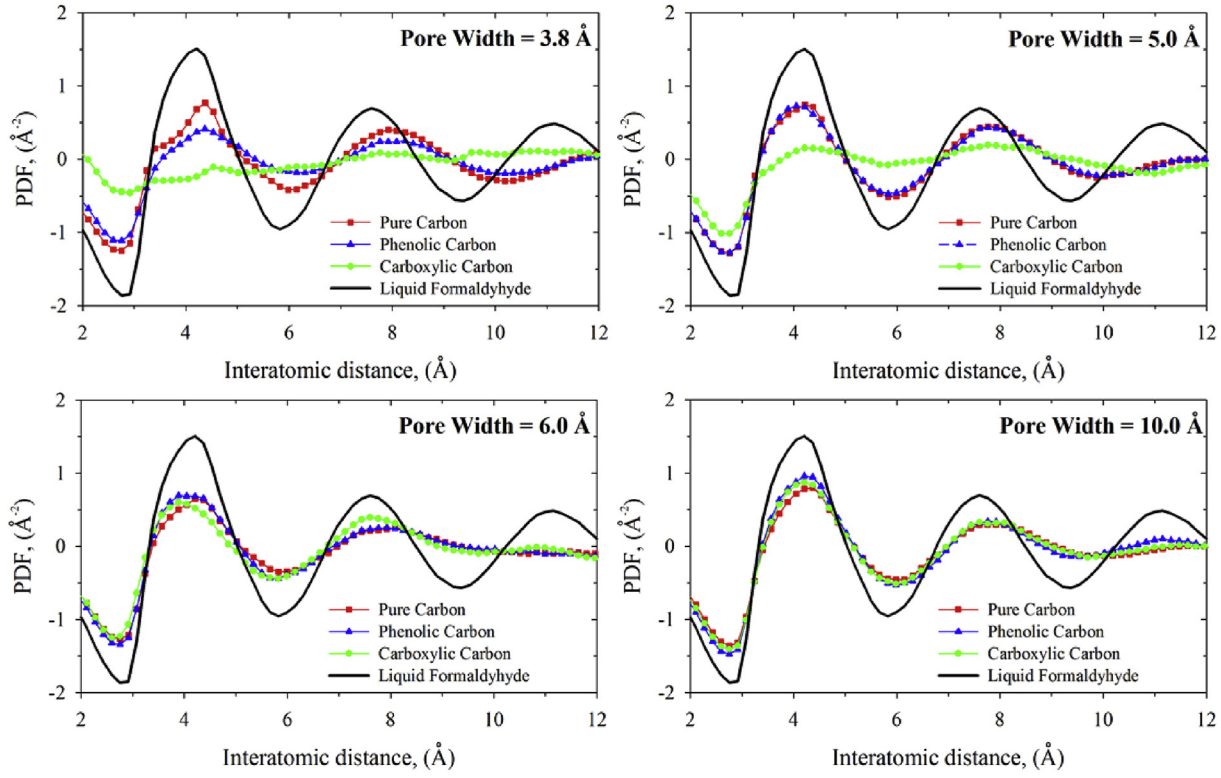

Fig. 6. Total X-ray pair correlation functions computed from the equilibrium configurations of formaldehyde adsorbed in 3.8, 5.0, 6.0, 7.2 and 10 Å pure/oxidized carbons at 2 atm and 303 K. For comparison, total X-ray pair correlation function computed for liquid formaldehyde (i.e., 0.816 g/cm^3) at 253 K is shown by solid line. (A colour version of this figure can be viewed online.)

~5.8 Å (a single layer of formaldehyde molecules, Fig. 4S, middle panel in the supporting information).

Fig. 6 displays the total X-ray pair correlation functions (TPCF) computed from the equilibrium configurations of formaldehyde adsorbed in 3.8, 5.0, 6.0, 7.2 and 10 Å pure/oxidized carbons at 2 atm and 303 K, which corresponds to micropores fully filled with formaldehyde (Figs. 2S–5S in the supporting information). For carboxylic carbons with narrow 3.8–5.0 Å ultramicropores, TPCF shows dramatic loss of the intermolecular correlations at short and long distances because irregular clusters of formaldehyde are randomly distributed between carboxylic groups. TPCF computed for carboxylic carbon with ~6 Å ultramicropores is very similar to TPCF computed for pure and phenolic carbons with ~6 Å ultramicropores, indicating similar structure of adsorbed formaldehyde in those carbons. In contrast, TPCF computed for formaldehyde adsorbed in pure and phenolic carbons with 3.8 Å ultramicropores have oscillatory character due to short-range intermolecular correlations. We notice that for all confined formaldehyde peak intensities on TPCF are decreased as a result of the reduced number of neighbors in quasi-two dimensional monolayers (Fig. 6). However, what is more interesting, we find that correlation peaks are broadening and their maxima are shifted to larger distances as compared to liquid formaldehyde (Fig. 6). Notable shift to larger intermolecular distances, particularly in narrow ~3.8–5 Å ultramicropores, indicates lower density of confined formaldehyde (i.e., weaker intermolecular interactions) at 303 K compared to formaldehyde liquid at 253 K. We can speculate that small accessible volume in narrow ultramicropores restricts the degree of formaldehyde dipole movements that generate observed regularities. Phenolic groups do not change the packing of formaldehyde significantly. Very high efficiency factor of phenolic carbon ultramicropores ~3.0–4.2 Å computed at zero-coverage is explained by the accessibility of the phenolic groups and strong H-bonding with formaldehyde. These results suggest that phenolic groups attached to graphitic pore walls do not induce blocking effects in narrow carbon ultramicropores, whereas carboxylic groups do induce excluded volumes and pore blocking.

To bridge the molecular modeling with experiment, we selected two strictly microporous (pore widths <20 Å [5], Fig. 7) samples of pitch-based ACF for experimental investigations of formaldehyde breakthrough using in-house apparatus (Fig. 1S in the supporting information). ACF 5 Å is a typical carbon molecular sieve (CMS) with a rationally tuned structure of ultramicropores (pore widths <7 Å [5]). ACF 7 Å has bimodal structure of micropores with a significant fraction of wider micropores, classified as supermicropores (7 Å < pore widths < 20 Å [5], Fig. 7(b)). We used hydrogen treatment and oxidation with perhydrol to generate four samples of ACF (Section 1.1). We treated pure ACF samples with

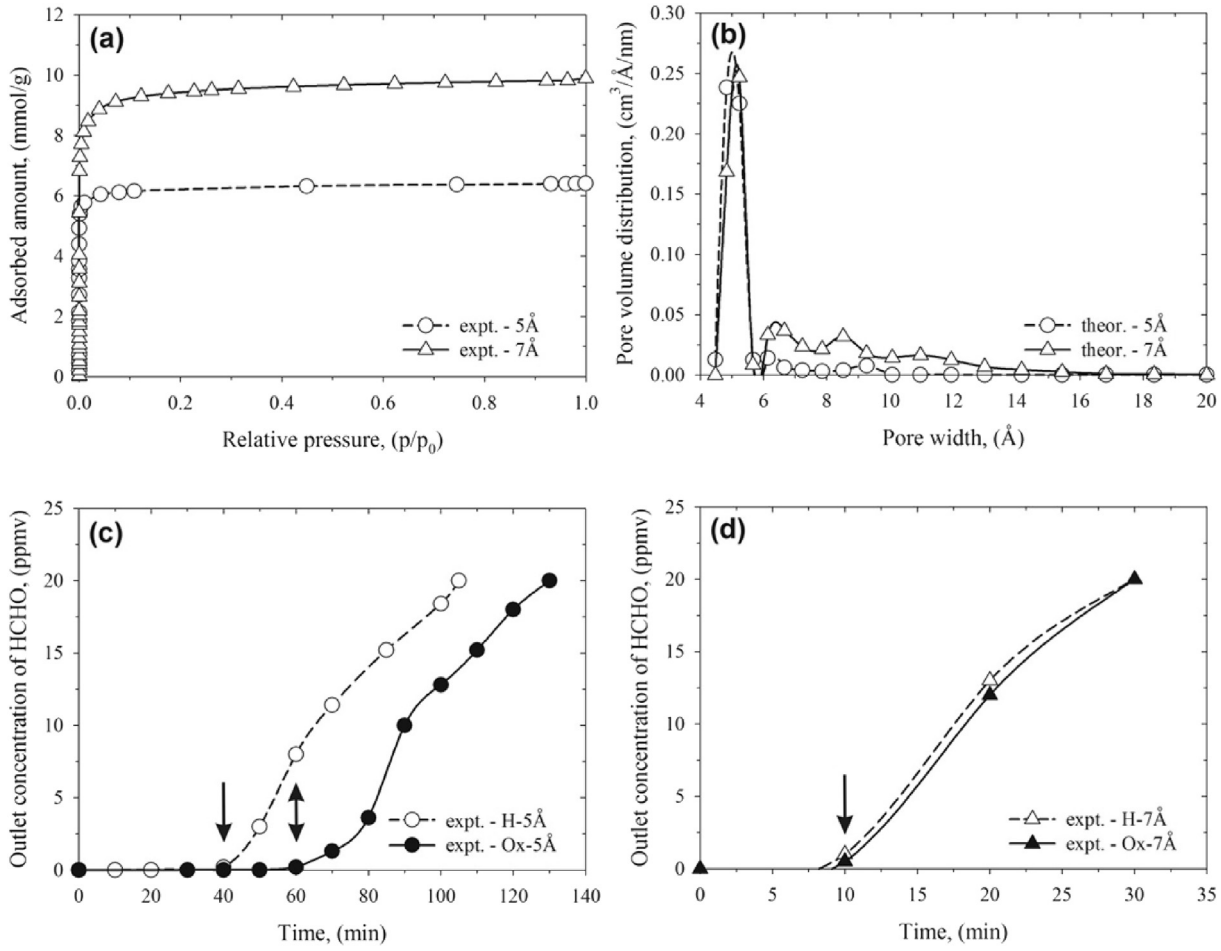

Fig. 7. (a) Experimental nitrogen adsorption isotherms measured for pitch-based microporous ACF 5 Å and 7 Å at 77.4 K. (b) QSDFT differential pore size distributions computed from nitrogen adsorption isotherms using slit-shaped carbon pore model. Breakthrough curves measured at the formaldehyde concentration of 20 ppm in nitrogen over hydrogen treated (-H) and oxidized (-Ox) 5 Å (c) and 7 Å (d) ACF fixed-beds at 303 K. The arrows show the breakthrough time of formaldehyde. It is worth noting that, because the experiments are performed at ppm concentrations, the breakthrough time on chemically modified ACFs is correlated with the binding efficiency characterized by the Henry factor rather than with the total adsorption capacity or with the accessible pore volume.

hydrogen at mild conditions to reduce the number of oxygen-containing functional groups without introduction of significant changes into micropore structure. We used mild oxidation with 10% perhydrol rather than boiling concentric nitric acid to introduce surface oxygen groups, predominantly phenolic and carboxylic, without any drastic modifications of micropore structure of ACF. Oxidation with perhydrol eliminates the formation of other surface groups with non-oxygen impurities (e.g. nitrates, nitrides, pyridine, etc.), which can impact on the breakthrough time of formaldehyde. Breakthrough curves obtained at the formaldehyde concentration of 20 ppm in nitrogen over hydrogen treated and oxidized ACF fixed beds at 303 K are presented in Fig. 7(b)-(d). Two striking features of formaldehyde breakthrough experiments are clearly apparent. First, we note that the column packed with hydrogen-treated ACF 5 Å adsorbent provides ~4 times longer protection against highly diluted formaldehyde compared to the column packed with hydrogen-ACF 7 Å adsorbent. Both hydrogen treated ACF samples contain ~4 wt % of oxygen (Table 1S in the supporting information), thus, we can assume a similar number of oxygen-containing functional groups (predominantly phenolic and carboxylic [26]) on micropore walls of 5 Å and 7 Å ACF samples. The drastic impact of the micropore size (i.e. a shift of pore size by ~2 Å) on the formaldehyde breakthrough is clearly evident. This experimental result is in agreement with high efficiency factor of formaldehyde in oxidized over pure ultramicropores (~<6 Å) computed at zero-coverage (Fig. 2). The longer breakthrough time indicates stronger binding of formaldehyde in ~5 Å carbon ultramicropores doped with ~4 wt % of oxygen at ~ ppm concentrations, as we find in molecular simulations. Therefore, the dynamic capacity of ACF 5 Å adsorbent is significantly improved as compared to ACF 7 Å adsorbent. Additional doping of ACF with oxygen (i.e., mild oxidation using 10% perhydrol) has profound impact on the formaldehyde breakthrough time measured for the column packed with oxidized ACF 5 Å adsorbent. The protection time against formaldehyde is further increased by ~20 min, indicating the cooperative effects of 5 Å ultramicropores and surface oxygen chemistry. On the contrary, the oxidation of carbon has negligible impact on the formaldehyde breakthrough time measured for the column packed with ACF 7 Å adsorbent. Indeed, molecular modeling shows that oxidation of carbon pore walls of larger micropores does not improve the efficiency factor of oxidized over pure carbons significantly (Fig. 2).

4. Conclusions

In this work, we have investigated the microscopic mechanism of formaldehyde adsorption in structural models of pure and oxidized carbons at 303 K, revealing cooperative effects of micropore size and surface oxygen chemistry on capture of formaldehyde at ~ ppm concentrations. From molecular modeling, we find large efficiency factor of formaldehyde in ~5.8 Å and ~3.0–4.0 Å ultramicropores oxidized with carboxylic and phenolic groups over pure ultramicropores, respectively (Fig. 2), which can be explained by formation of H-bonds between formaldehyde and surface functional groups. Furthermore, we find the excluded volume effects in narrow ultramicropores generated by carboxylic groups that leads to the dramatic decrease of formaldehyde capture in carboxylic carbons with narrow 3.0–4.0 Å ultramicropores. Oxidation of supermicropores and narrow mesopores with pore size ~>7.0 Å has a negligible impact on the capture of highly diluted formaldehyde, that can be explained by reduction of the number of H-bonds of formaldehyde with oxygen-containing functional groups (Fig. 5). Experimental measurements of breakthrough time of formaldehyde through pure and oxidized ACF packed bed column confirm the simulation predictions and show that oxidized nanocarbons with optimized pore size ~<6 Å have a great potential for highly diluted formaldehyde capture (Fig. 7). This study is a promising example of the use of molecular modeling for *in-silico* screening and design of optimal nanoporous carbon adsorbents for air purification from highly diluted toxic industrial chemicals.

Acknowledgments

Piotr A. Gauden and Sylwester Furmaniak acknowledge the use of the computer cluster at Poznań Supercomputing and Networking Centre (Poznań, Poland). Piotr Kowalczyk thanks Prof. Andrzej Burian (A. Chelkowski Institute of Physics, University of Silesia, Poland) for fruitful comments on the wide-angle X-ray scattering theory. KK is partially supported by Grant-in-aid (B)(17H03039). AVN acknowledges partial support from the NSF Rutgers ERC on Structured Organic Particulate Systems. This work is dedicated to the memory of Professor Ian Snook (RMIT University, Australia) for his impact on the field of statistical mechanics of soft condensed matter systems.

Appendix A. Supplementary data

Supplementary data related to this article can be found at http://dx.doi.org/10.1016/j.carbon.2017.08.024.

References

[1] G. Hantal, P. Jedlovszky, P.N.M. Hoang, S. Picaud, Calculation of the adsorption isotherm of formaldehyde on ice by grand canonical Monte Carlo simulation, J. Phys. Chem. C 111 (2007) 14170–14178.
[2] AFSSET, Risques sanitaires liés à la présence de formaldéhyde, Saisine n° 2004/16, 2008, http://www.anses.fr.
[3] K.J. Lee, J. Miyawaki, N. Shiratori, S.-H. Yoon, J. Jang, Toward an effective adsorbent for polar pollutants: formaldehyde adsorption by activated carbon, J. Hazard Mater. 260 (2013) 82–88.
[4] K.J. Lee, N. Shiratori, G.H. Lee, J. Miyawaki, I. Mochida, S.-H. Yoon, J. Jang, Activated carbon nanofiber produced from electrosupn polyacrylonitrile nanofiber as a highly efficient formaldehyde adsorbent, Carbon 48 (2010) 4248–4255.
[5] M. Thommes, K. Kaneko, A.V. Neimark, J.P. Olivier, F. Rodriguez-Reinoso, J. Rouquérol, et al., Physisorption of gases, with special reference to the evaluation of surface area and pore size distribution (IUPAC Technical Report), Pure Appl. Chem. 87 (2015) 1051–1069.
[6] Y. Matsuo, Y. Nishino, T. Fukutsuka, Y. Sugie, Removal of formaldehyde from gas phase by silylated graphite oxide containing amino groups, Carbon 46 (2008) 1159–1174.
[7] V. Boonamnuayvitaya, S. Sae-ung, W. Tanthapanichakoonchakoon, Preparation of activated carbons from coffee residue for the adsorption of formaldehyde, Sep. Purif. Technol. 42 (2005) 159–168.
[8] Y. Song, W. Qiao, S.-H. Yoon, I. Mochida, Q. Guo, L. Liu, Removal of formaldehyde at low concentration using various activated carbon fibers, J. App. Polym. Sci. 106 (2007) 2151–2157.
[9] H.B. An, M.J. Yu, J.M. Kim, M. Jin, J.-K. Jeon, S.H. Park, S.-S. Kim, Y.-K. Park, Indoor formaldehyde removal over CMK-3, Nanoscale Res. Lett. 7 (2012) 1–6.
[10] E.M. Carter, L.E. Katz, G.E. Speitel, D. Ramirez, Gas-phase formaldehyde adsorption isotherm studies on activated carbon: correlations of adsorption capacity to surface functional group density, Environ. Sci. Technol. 45 (2011) 6498–6503.
[11] R. Ch Bansal, M. Goyal, Activated Carbon Adsorption, CRC Press, Boca Raton, 2005.
[12] A.P. Terzyk, G. Rychlicki, M.S. Ćwiertnia, P.A. Gauden, P. Kowalczyk, Effect of carbon surface layer chemistry on benzene adsorption from the vapour phase and from dilute aqueous solutions, Langmuir 21 (2005) 12257–12267.
[13] P.I. Ravikovitch, A. Vishnyakov, R. Russo, A.V. Neimark, Unified approach to pore size characterization of microporous carbonaceous materials from N_2, Ar, and CO_2 adsorption isotherms, Langmuir 16 (2000) 2311–2320.
[14] J.C. Palmer, J.K. Brennan, M.M. Hurley, A. Balboa, K.E. Gubbins, Detailed structural model for activated carbons from molecular simulation, Carbon 47 (2009) 2904–2913.
[15] T.X. Nguyen, N. Cohaut, J.-S. Bae, S.K. Bhatia, New method for atomistic modelling of the microstructure of activated carbons using hybrid reverse Monte Carlo simulation, Langmuir 24 (2008) 7912–7922.
[16] S.H. Madani, Ch Hu, A. Silvestre-Albero, M.J. Biggs, F. Rodríguez-Reinoso, P. Pendleton, Pore size distributions derived from adsorption isotherms, immersion calorimetry, and isosteric heats: A comparative study, Carbon 96 (2016) 1106–1113.

[17] H. Marsh, F. Rodríguez-Reinoso, Activated Carbon, Elsevier Ltd., London, 2006.
[18] M. Thommes, K. Cychosz, A.V. Neimark, Advanced physical adsorption characterization of nanoporous carbons, in: J.M.D. Tascon (Ed.), Novel Carbon Adsorbents, Elsevier Ltd., London, 2012, pp. 107–145.
[19] P. Kowalczyk, A.P. Terzyk, P.A. Gauden, R. Leboda, E. Szmechting-Gauden, G. Rychlicki, Z. Ryu, H. Rong, Estimation of the pore size distribution from nitrogen adsorption isotherm. The comparison of density functional theory and the method of Do and co-workers, Carbon 41 (2003) 1113–1125.
[20] J. Jagiello, M. Thommes, Comparison of DFT characterization methods based on N_2, Ar, CO_2, and H_2 adsorption applied to carbons with various pore size distributions, Carbon 42 (2004) 1227–1232.
[21] Ch Lastoskie, K.E. Gubbins, N. Quirke, Pore size distribution analysis of microporous carbons: A density functional theory approach, J. Phys. Chem. 97 (1993) 4786–4796.
[22] P. Kowalczyk, A.P. Terzyk, P.A. Gauden, S. Furmaniak, M. Wiśniewski, A. Burian, L. Hawelek, K. Kaneko, A.V. Neimark, Carbon molecular sieves: reconstruction of atomistic structural models with experimental constrains, J. Phys. Chem. C 118 (2014) 12996–13007.
[23] M. Jaroniec, R.K. Gilpin, K. Kaneko, Evaluation of energetic heterogeneity and microporosity of activated carbon fibers on the basis of gas adsorption isotherms, Langmuir 7 (1991) 2719–2722.
[24] P. Kowalczyk, K. Kaneko, A.P. Terzyk, H. Tanaka, H. Kanoh, P.A. Gauden, The evaluation of the surface heterogeneity of carbon blacks from the lattice density functional theory, Carbon 42 (2004) 1813–1823.
[25] W. Rudzinski, D.M. Everett, Adsorption of Gases on Heterogeneous Surfaces, Academic Press, London, 1992.
[26] H.P. Boehm, E. Diehl, W. Heck, R. Sappok, Surface oxides of carbon, Angew. Chem. Int. Ed. 3 (1964) 669–677.
[27] T.J. Bandosz (Ed.), Activated Carbon Surfaces in Environmental Remediation, Elsevier, Amsterdam, 2006.
[28] Q. Wen, C. li, Z. Cai, W. Zhang, H. Gao, L. Chen, G. Zeng, X. Shu, Y. Zhao, Study on activated carbon derived from sewage sludge for adsorption of gaseous formaldehyde, Bioresour. Technol. 102 (2011) 942–947.
[29] J. Miyawaki, T. Kanda, K. Kaneko, Hysteresis-associated pressure-shift-induced water adsorption in carbon micropores, Langmuir 17 (2001) 664–669.
[30] K. Kaneko, Y. Hanzawa, T. Iiyama, T. Kanda, T. Suzuki, Cluster-mediated water adsorption on carbon nanopores, Adsorption 5 (1999) 7–13.
[31] P. Kowalczyk, H. Tanaka, R. Holyst, K. Kaneko, T. Ohmori, J. Miyamoto, Storage of hydrogen at 303 K in graphite slitlike pores from grand canonical Monte Carlo simulation, J. Phys. Chem. B 109 (2005) 17174–17183.
[32] S. Furmaniak, A.P. Terzyk, P.A. Gauden, P.J.F. Harris, P. Kowalczyk, Can carbon surface oxidation shift the pore size distribution curve calculated from Ar, N_2 and CO_2 adsorption isotherms? Simulation results for a realistic carbon model, J. Phys. Condens. Matter 21 (2009) 315005–315015.
[33] S. Furmaniak, P. Kowalczyk, A.P. Terzyk, P.A. Gauden, P.J.F. Harris, Synergetic effect of carbon nanopore size and surface oxidation on CO_2 capture from CO_2/CH_4 mixtures, J. Coll. Interf. Sci. 397 (2013) 144–153.
[34] W. Humphrey, A. Dalke, K. Schulten, VMD - visual molecular dynamics, J. Molec. Graph. 14.1 (1996) 33–38.
[35] D. Nicholson, N.G. Parsonage, Computer Simulation and Statistical Mechanics of Adsorption, Academic Press, London, 1982.
[36] P. Kowalczyk, P.A. Gauden, A.P. Terzyk, A.V. Neimark, Screening of carbonaceous nanoporous materials for capture of nerve agents, Phys. Chem. Chem. Phys. 15 (2013) 291–298.
[37] W.L. Jorgensen, D.S. Maxwell, J. Tirado-Rives, Development and testing of the OPLS all-atom force field on conformational energetics and properties of organic liquids, J. Am. Chem. Soc. 118 (1996) 11225–11236.
[38] M.P. Allen, D.J. Tildesley, Computer Simulation of Liquids, Clarendon, Oxford, 1987.
[39] A. Vishnyakov, A.V. Neimark, Studies of liquid-vapor equilibria, criticality, and spinodal transitions in nanopores by the gauge cell Monte Carlo simulation method, J. Phys. Chem. B 105 (2001) 7009–7020.
[40] P. Kowalczyk, R. Holyst, H. Tanaka, K. Kaneko, Distribution of carbon nanotube sizes from adsorption measurements and computer simulation, J. Phys. Chem. B 109 (2005) 14659–14666.
[41] M.C. Gordillo, J. Martí, Hydrogen bond structure of liquid water confined in nanotubes, Chem. Phys. Lett. 329 (2000) 341–345.
[42] M. Wiśniewski, S. Furmaniak, A.P. Terzyk, P.A. Gauden, P. Kowalczyk, Properties of phenol confined in realistic carbon micropore model: experiment and simulations, J. Phys. Chem. C 119 (2015) 19987–19995.
[43] K. Jurkiewicz, L. Haweł ek, K. Balin, J. Szade, F.L. Braghiroli, V. Fierro, A. Celzard, A. Burian, Conversion of natural tannin to hydrothermal and graphene-like carbons studied by wide-angle X-ray scattering, J. Phys. Chem. A 119 (2015) 8692–8701.
[44] O. Madejczyk, K. Kaminski, E. Kaminska, K. Jurkiewicz, M. Tarnacka, A. Burian, M. Paluch, Interplay between the static ordering and dynamical heterogeneities determining the dynamics of rotation and ordinary liquid phases in 1,6-anhydro-β-D-glucose, Sci. Rep. 7 (2017) 42103.
[45] A.V. Neimark, P.I. Ravikovitch, A. Vishnyakov, Inside the hysteresis loop: multiplicity of internal; states of confined fluids, Phys. Rev. E 65 (2002) 031505.
[46] A. Striolo, A.A. Chialvo, P.T. Cummings, K.E. Gubbins, Water adsorption in carbon-slit nanopores, Langmuir 19 (2003) 8583–8591.
[47] J.C. Liu, P.A. Monson, F. van Swol, Studies of a lattice model of water confined in a slit pore, J. Phys. Chem. C 111 (2007) 15976–15981.
[48] L. Sarkisov, A. Centineo, S. Brandani, Molecular simulation and experiments of water adsorption in a high surface area activated carbon: hysteresis, scanning curves and spatial organization of water clusters, Carbon 118 (2017) 127–138.
[49] S. Furmaniak, P.A. Gauden, A.P. Terzyk, G. Rychlicki, Water adsorption on carbons-critical review of the most popular analytical approaches, Adv. Colloid Interface Sci. 137 (2008) 82–143.
[50] T. Ohba, H. Kanoh, K. Kaneko, Cluster-growth-induced water adsorption in hydrophobic carbon nanopores, J. Phys. Chem. B 108 (2004) 14964–14969.
[51] G.R. Birkett, D.D. Do, Simulation study of water on carbon black: the effect of graphite water interaction strength, J. Phys. Chem. C 111 (2007) 5735–5742.